

PIN Diode Switching Speed for MRI Applications

Robert H. Caverly

ECE Department

Villanova University

Villanova, PA USA

ORCID: 0000-0002-9212-7660

Abstract— This paper presents the results of an investigation of PIN diode switching speed using a variety of PIN diode types that include high speed receive switching devices as well as high power transmitting PIN diodes. A short introduction on the PIN diode simulation model will be provided and then simulations of a common MRI transmit/receive switch will be used to compare the different device switching speeds. The results show that thick I-region diodes are shown to exhibit extremely low resistance values at high currents, providing low insertion loss at the high RF powers in transmitting, active detune and block switching applications as well as robust blocking/detuning functions, but at a slower switching rate compared with thinner devices.

Keywords— *magnetic resonance imaging, PIN diode, switching*

I. INTRODUCTION

Magnetic resonance imaging (MRI) scanners are sophisticated diagnostic instruments consisting partly of a radio frequency (RF) section that requires tight timing control. Both transmit and receive signals must be switched, steered, or blocked according the pulsing sequence, and these actions must often take place within microseconds (μ s). With the high powers involved in the MRI RF portion of the imaging process, mechanical switching can be done but the switching speed is slow and so solid-state control is required. There are several solid-state device options that can be used such as MEMS or FETs, but for the high power, high speed response, the PIN diode is often the switching device of choice. On the transmit side, the PIN diode can be used to help control the pulse shape, switch in various transmit coil sections for a multi-band transmit coil or be used in automated coil matching structures. In these applications, the PIN diode is in the high-power RF path. To handle these power levels, the PIN diodes themselves are physically large, with I-region thicknesses (W) exceeding 200 micrometers (μ m) and with cross sections that yield off-state capacitances in the picofarads. In general, large W PIN diodes often have I-region carrier lifetimes (τ) that are in the microseconds range. With DC bias currents in the hundreds of milliAmperes (mA), the I-region of these devices can store considerable charge that must be removed (injected) when the device is being turned off (on) which can take tens of microseconds or longer depending on the driver circuit. On the receive side, PIN diodes are often used in a similar fashion as microwave limiters to reduce the RF energy at the input to sensitive low noise amplifiers, or to detune RF receive coils away from the Larmor frequency during the high power transmit pulse. In both cases, the RF powers or voltages are significantly less than the transmit RF path, but these devices also must operate at high speed to quickly switch from their

inactive to active state. This usually requires thin W and short τ devices so that the injected (removed) charge during the state change is small. For these applications, the diode is usually operated in its so-called passive state, where the injected or removed charge is usually obtained through self-rectification of the device from the applied RF signal.

This paper presents the results of an investigation of PIN diode switching speed using a variety of PIN diode types that include high speed receive switching devices as well as high power transmitting PIN diodes. A short introduction on the PIN diode simulation model will be provided and then simulations of a common MRI transmit/receive (T/R) switch will be used to compare the different device switching speeds.

II. SIMULATION MODEL

A. Time-Domain PIN Diode Model

The simulations are based on a time-domain model for the PIN diode that is based on the underlying physics of the diode's operation and can be implemented in a SPICE-like circuit simulator [1]. This model has more recently been incorporated into several commercial circuit simulators and will be used in this work. The model uses dependent sources to simulate the injected charge in the I-region as well as the impact of the PN junctions on the current-voltage as well as frequency characteristics of the device. Fig. 1 shows the basic model layout in equivalent circuit form, where G_{PN} simulates the PN junction effects and G_{mod} simulates the conductivity modulation in the I-region by the injected current. The remaining lumped elements in the equivalent circuit model are the PIN diode parasitics such as bond wire inductance L_{bond} and package capacitance C_{pack} .

B. Test Circuit: MRI Transmit/Receive Switch

The test circuit used in this study is based on the classic linear balanced duplexer outlined in the classic MIT Radiation Laboratory series [2] and further used in [3] and is shown in Fig. 2. The circuit operates as follows: if the PIN diodes (Z_{CTL}) are turned on, they ideally represent a short circuit at the output of the first quadrature hybrid and all energy from the transmitter (Source) is reflected at the diode connection point. There is no power dissipation in PIN diodes (in the ideal case); however, in a real circuit, the diodes would exhibit a low value of resistance, causing the PIN diodes to dissipate power.

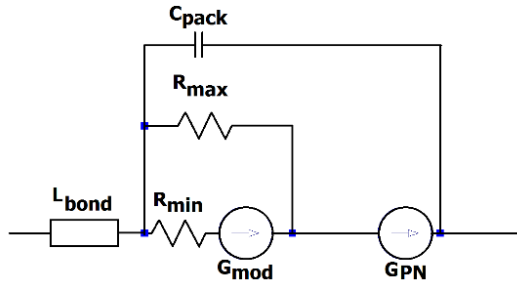


Fig. 1. PIN diode model used in the work [1].

For this on-state case, the PIN diodes would need to be physically large to handle the large RF power at that point, and hence a large W , long τ device would be required. When the diodes are off, $\Gamma=0$ and energy goes through the hybrids and appears at the output ports outA and outB; the receive LNA would be attached to the circuit at point outA.

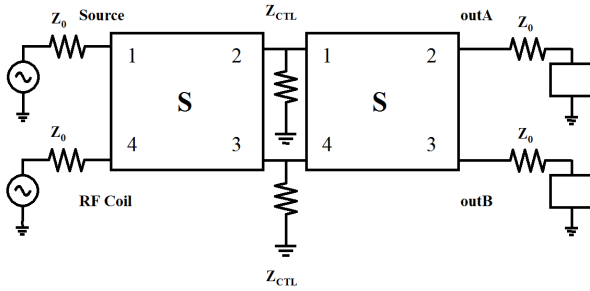


Fig. 2. Schematic diagram of the T/R switch used in the study. Z_{CTL} represents the PIN diode [3].

Eqn. 1 shows the S-parameters of the T/R switch at the three output ports [3]:

$$\frac{V_{outA}}{V_{Source}} = S_{BA} = (1 + \Gamma) \left[S_{21} \frac{S_{21} + \Gamma S_{23} S_{31}}{1 - \Gamma^2 S_{23} S_{32}} + S_{24} \frac{S_{31} + \Gamma S_{32} S_{21}}{1 - \Gamma^2 S_{23} S_{32}} \right] \quad (1a)$$

$$\frac{V_{outA}}{V_{RF-Coil}} = S_{BD} = (1 + \Gamma) \left[S_{21} \frac{S_{24} + \Gamma S_{23} S_{34}}{1 - \Gamma^2 S_{23} S_{32}} + S_{24} \frac{S_{34} + \Gamma S_{32} S_{24}}{1 - \Gamma^2 S_{23} S_{32}} \right] \quad (1b)$$

$$\frac{V_{RF-Coil}}{V_{Source}} = S_{DA} = S_{41} + \Gamma \left[S_{42} \frac{S_{21} + \Gamma S_{23} S_{31}}{1 - \Gamma^2 S_{23} S_{32}} + S_{43} \frac{S_{31} + \Gamma S_{32} S_{21}}{1 - \Gamma^2 S_{23} S_{32}} \right] \quad (1c)$$

where the S_{ij} are the S-parameters for the two quadrature hybrids and Γ is the reflection coefficient caused by the two diodes at the junction of the two hybrids. The results of (1) show that PIN diodes with lower resistance exhibit both low insertion loss from the transmitter to the coil but also high isolation between the transmitter and the LNA (Fig. 3). However, as the PIN diode resistance increases, increased power dissipation by the device will also occur, which must be a factor in considering the I-region thickness W and the level of DC forward current to be applied to the diode.

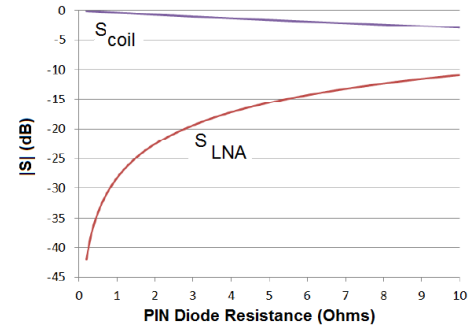


Fig. 3. S-parameters between the transmitter and the coil (S_{coil}) and low noise amplifier (S_{LNA}).

III. SIMULATIONS

A. Basic circuit structure

To show the utility of the model and T/R switch arrangement to MR circuit designers, the T/R switch circuit in Fig. 4 was implemented in a simulator using $\lambda/8$ lines and shunt-connected capacitors to implement each quadrature hybrid. The test frequency was 298 MHz, corresponding to the 7 T Larmor frequency for ^1H (hydrogen), the most frequently imaged atomic species. All ports were terminated in matched loads and the source exhibited a 50 Ohm impedance. DC bias was applied through an inductor using a switched DC voltage supply and current limiting resistor to simulate the PIN diode driver circuit. A pulse width of 10 μs was used to investigate the switching speed of the devices for MRI scanning using short-pulse techniques. Pulse repetition rate TR was set to 60 μs in the simulations (Fig. 4). The start of the echo time TE period would depend on the switching speed of the PIN diodes when they reached their final switched state. In Fig. 4, from 0-10 μs and 60-70 μs , the PIN diodes are in their on-state and the blue waveform indicates the signal at the LNA port during the transmit pulse is more than 40 dB down from the transmit/source port, indicating a PIN diode on-state resistance of less than one Ohm, which is consistent with the traditional on-state resistance equation for PIN diodes:

$$R = W^2 / 2\mu \tau I_{DC} \quad (2)$$

where μ is the ambipolar mobility, $W=40 \mu\text{m}$ and $\tau = 2 \mu\text{s}$ for the device used in this example. During the pulse period 10-50 μs , the PIN diodes are off (-6 V reverse bias) and the signal from the coil to the receive port exhibits less than 0.1 dB insertion loss.

The impact of injected (extracted) stored charge during the diode turn on (off) phases can be studied by expanding Fig. 4 during the various signal transitions. Fig. 5 shows the signal at the LNA port (blue) during these two phases; note the difference in time scales. Fig. 5a shows that there is significant time delay between the signal rising to its final value at the LNA after the turn-off signal to the diodes has been sent (10 μs -10,000ns). This figure shows that with 60 mA reverse current applied during the turn-off phase, the delay time is approximately 1.3 μs before full signal is received.

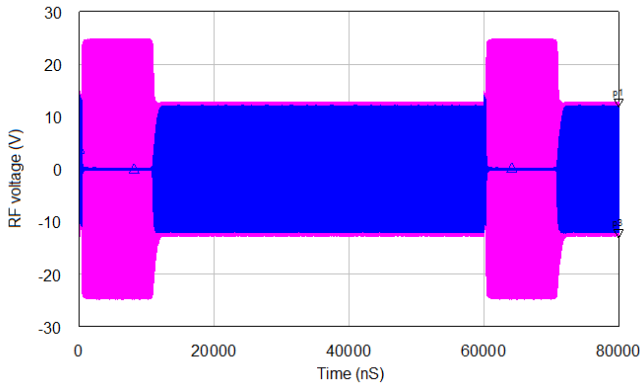


Fig. 4. Short-pulse sequence for MRI for investigation of PIN diode switching speed as a function of device parameters.

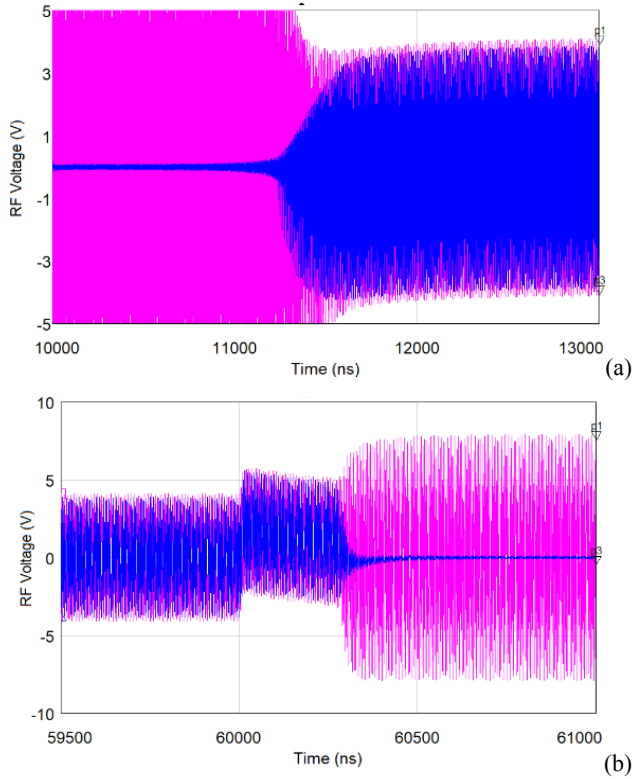


Fig. 5. Expanded view of the diode turn-on and turn-off phases in the MRI T/R switch: a) diode turn-off; b) diode turn-on.

In contrast, during the turn-on pulse (60 μ s) waveform shown in Fig. 5b, the signal achieves full isolation in less than 400 ns. To show the benefit of a larger reverse current to reduce switching speed, Fig. 6 shows the same circuit except with approximately 150 mA of reverse current applied during the off-state transition. In this case, the low insertion loss signal occurs within 750 ns of the application of the turn-off pulse, indicating higher reverse currents during switching transitions will greatly improve PIN diode switching speeds. Table 1 summarizes the

results of simulations of the turn on/off delay of PIN diodes of several different geometries and electrical characteristics. Thin PIN diodes are usually used in lower power applications such as with receiver coils, whereas the thicker devices are typically reserved for use in the high-power RF transmit path. Note the thinner devices exhibit faster switching speeds, especially when switching to the off- state, because of the reduced stored charge needed in the I-region that must be extracted or injected.

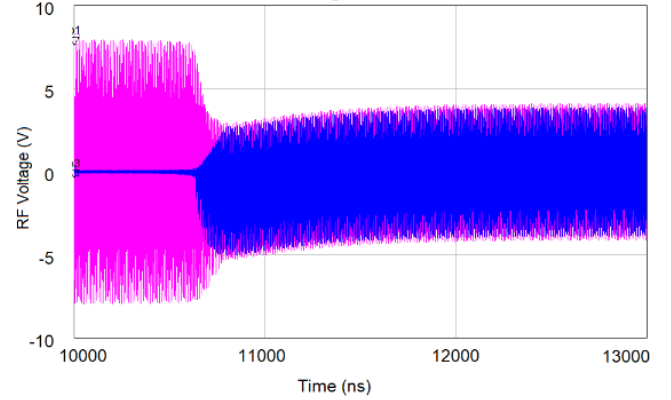


Fig. 6. Expanded view of the diode turn-off phases in the MRI T/R switch.

TABLE 1. RESULTS OF SIMULATIONS OF THE T/R SWITCH WITH PIN DIODES OF VARIOUS W AND T VALUES.

W (μ m)	6	40	175
τ (μ s)	0.012	2	26
IDC(mA) (on/off)	100/-5	100/-5	200/-20
ON delay (μ s)	0.6	0.5	2
OFF delay (μ s)	1.2	9	33

IV. CONCLUSION

Higher power thick I-region diodes are shown to exhibit extremely low resistance values at high currents, providing low insertion loss at the high RF powers in transmitting, active detune and block switching applications as well as robust blocking/detuning functions, but at a somewhat slower switching rate compared with thinner devices due to the I-region stored charge.

REFERENCES

- [1] R. H. Caverly, N. V. Drozdovski, L. M. Drozdovskaia and M. J. Quinn, "SPICE modeling of microwave and RF control diodes," *Proceedings of the 43rd IEEE Midwest Symposium on Circuits and Systems* (Cat.No.CH37144), Lansing, MI, 2000, pp. 28-31 vol.1.
- [2] Smullin and Montgomery, *Microwave Duplexers*, Radiation Laboratory Series. v. 14 pp.150-352, 1948.
- [3] R. H. Caverly, "PIN diode-based transmit-receive switch for 7 T MRI," 2016 IEEE Topical Conference on Biomedical Wireless Technologies, Networks, and Sensing Systems (BioWireless2016), Austin, TX, 2016, pp. 100-102.